Tripathi et al., http://www.jcb.org/cgi/content/full/jcb.201405105/DC1

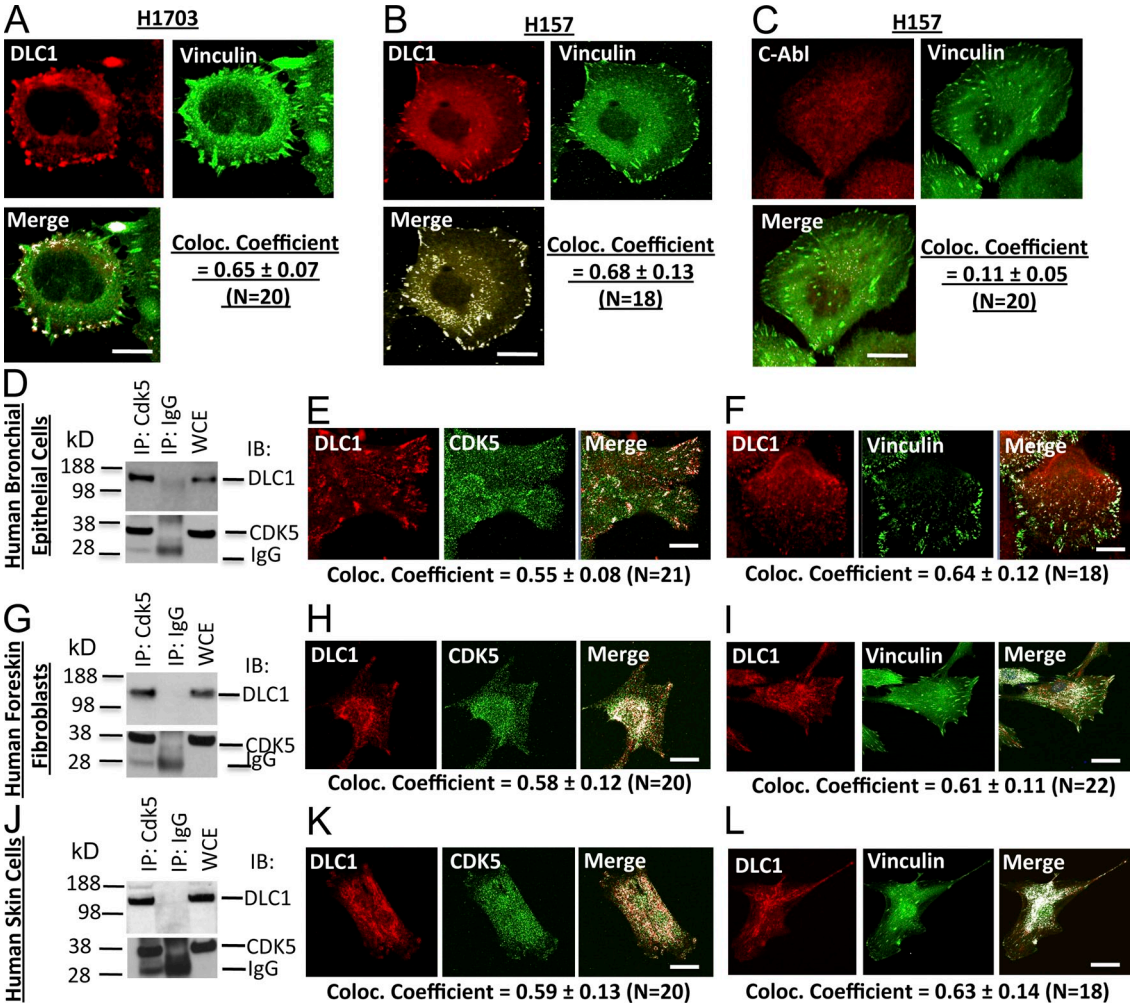

Figure S1. **DLC1 and CDK5 form an endogenous protein complex and colocalized in human cells.** (A) Colocalization of DLC1 with the focal adhesion protein Vinculin in H1703 cells. Cells were stained with DLC1 (red) and Vinculin (green) antibodies, and the colocalization between DLC1 and Vinculin is highlighted in white in the merge image. Images in the figure are representative of the majority of cells. An averaged overlapping colocalization coefficient ± SD was calculated from 20 cells randomly selected from several fields, and is shown on the bottom right of each section. (B) Experimental conditions were similar to those in A. Colocalization of DLC1 with the focal adhesion protein Vinculin in H157 cells. (C) Experimental conditions were similar to those in A. c-ABL protein does not colocalize with Vinculin at focal adhesions, and was used as a negative control. (D) Protein complex formation between DLC1 and CDK5 in HBEC cells. Cell lysates were immunoprecipitated (IP) with DLC1 antibody followed by IB with DLC1 (top) or CDK5 (bottom) antibodies. (E) Colocalization of endogenous DLC1 with CDK5; HBEC cells were stained with DLC1 (red) and CDK5 (green) antibodies, and the colocalization between DLC1 and CDK5 is highlighted in white in the merge image. (F) Experimental conditions were similar to E. Colocalization of endogenous DLC1 with Vinculin is shown. (G) Protein complex formation between DLC1 and CDK5 in human foreskin fibroblasts. Experimental conditions were as in D. (H) Colocalization of endogenous DLC1 with CDK5 in human foreskin fibroblasts. (I) Colocalization of endogenous DLC1 with Vinculin in human foreskin fibroblasts. (J) Protein complex formation between DLC1 and CDK5 in human skin cells. Experimental conditions were as in D. (K) Colocalization of endogenous DLC1 with CDK5 in human skin cells. (L) Colocalization of endogenous DLC1 with Vinculin in human skin. Images in the figure are representative of the majority of cells. An averaged overlapping colocalization coefficient ± SD was calculated from 18–22 cells in each group randomly selected from several fields, and is shown at the bottom of each panel. Bars, 20 µm.

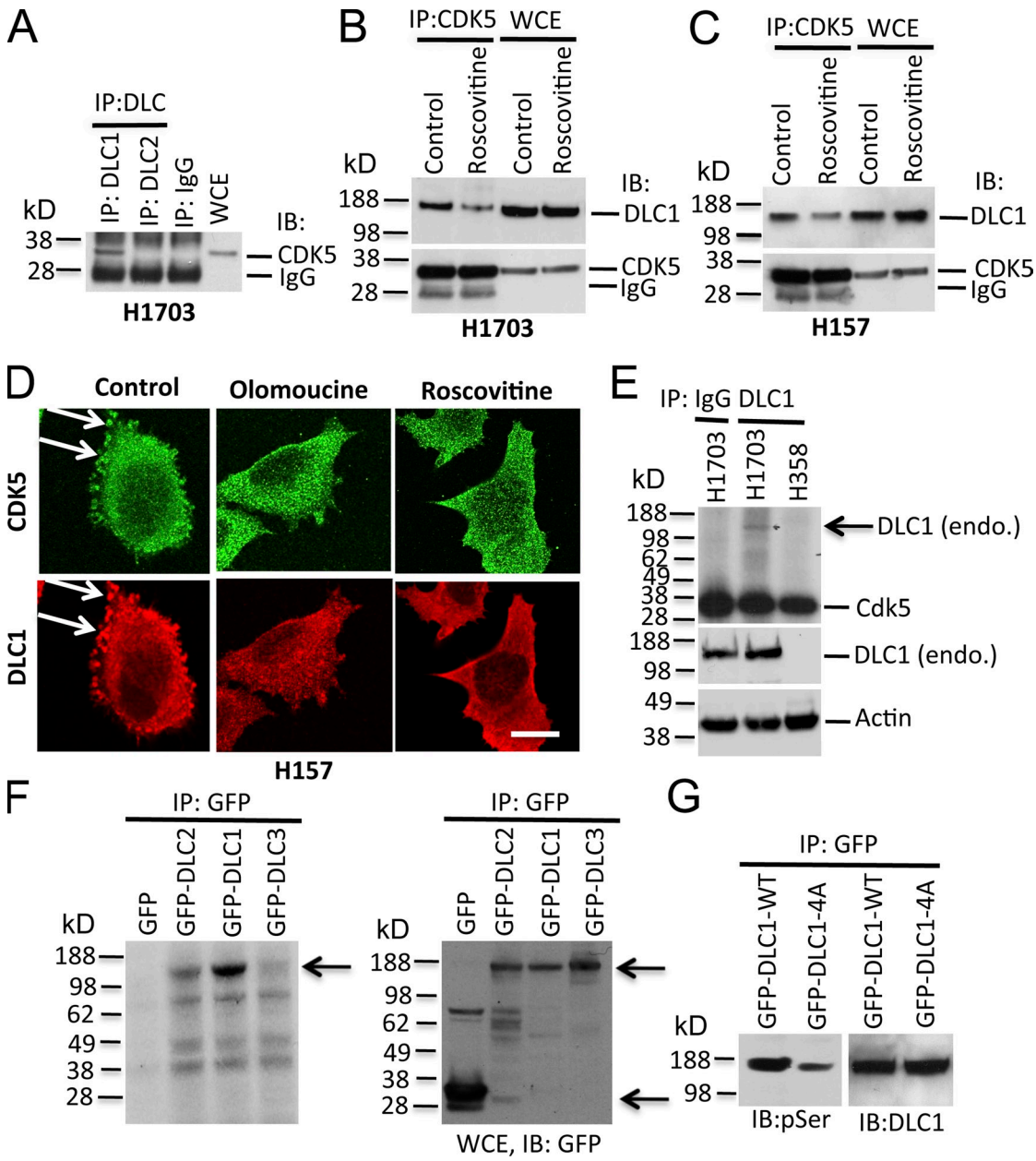

Figure S2. **Interaction of DLC1 and CDK5 requires the CDK5 kinase activity.** (A) Endogenous CDK5 forms a complex with DLC1 but not with DLC2. Lysates from H1703 cells were immunoprecipitated with DLC1, DLC2, or IgG followed by IB with CDK5 antibodies. (B) Roscovitine treatment inhibits complex formation between DLC1 and CDK5. Lysates from H1703 cells were immunoprecipitated with CDK5 antibody followed by IB with DLC1 antibody (top) and CDK5 antibody (bottom) in the absence or presence of Roscovitine. (C) Experimental conditions were similar to those in B. Roscovitine inhibits the complex formation between DLC1 and CDK5 in H157 cells. (D) CDK5 kinase inhibition by Olomoucine or Roscovitine reduced the punctate structures (arrows). Bar, 20 μm. Images in the figure are representative of the majority of cells. (E) CDK5 kinase phosphorylates endogenous DLC1. (top) DLC1 was immunoprecipitated from DLC1-positive H1703 cells, and is phosphorylated by recombinant CDK5 kinase; IP from DLC1-negative H358 cells has no phosphorylation signal. (middle) Endogenous expression of DLC1 in WCE of H1703, but not in H358. (bottom) Actin was used as the loading control. (F) Phosphorylation of DLC1, but not DLC2 or DLC3, by CDK5 was detected with ^{32}P autoradiography. (left) GFP-tagged DLC1, but not DLC2 and DLC3, is phosphorylated by recombinant CDK5 kinase (arrow). (right) Expression of GFP, GFP-DLC1, GFP-DLC2, and GFP-DLC3 were detected by GFP antibody in WCE. Arrows indicate the expressed proteins. (G) In vivo serine phosphorylation in the DLC1-4A mutant was substantially reduced compared to DLC1-WT. GFP-DLC1-WT or GFP-DLC1-4A were immunoprecipitated with GFP antibody and immunoblotted with pSer (left) or DLC1 (right) antibodies.

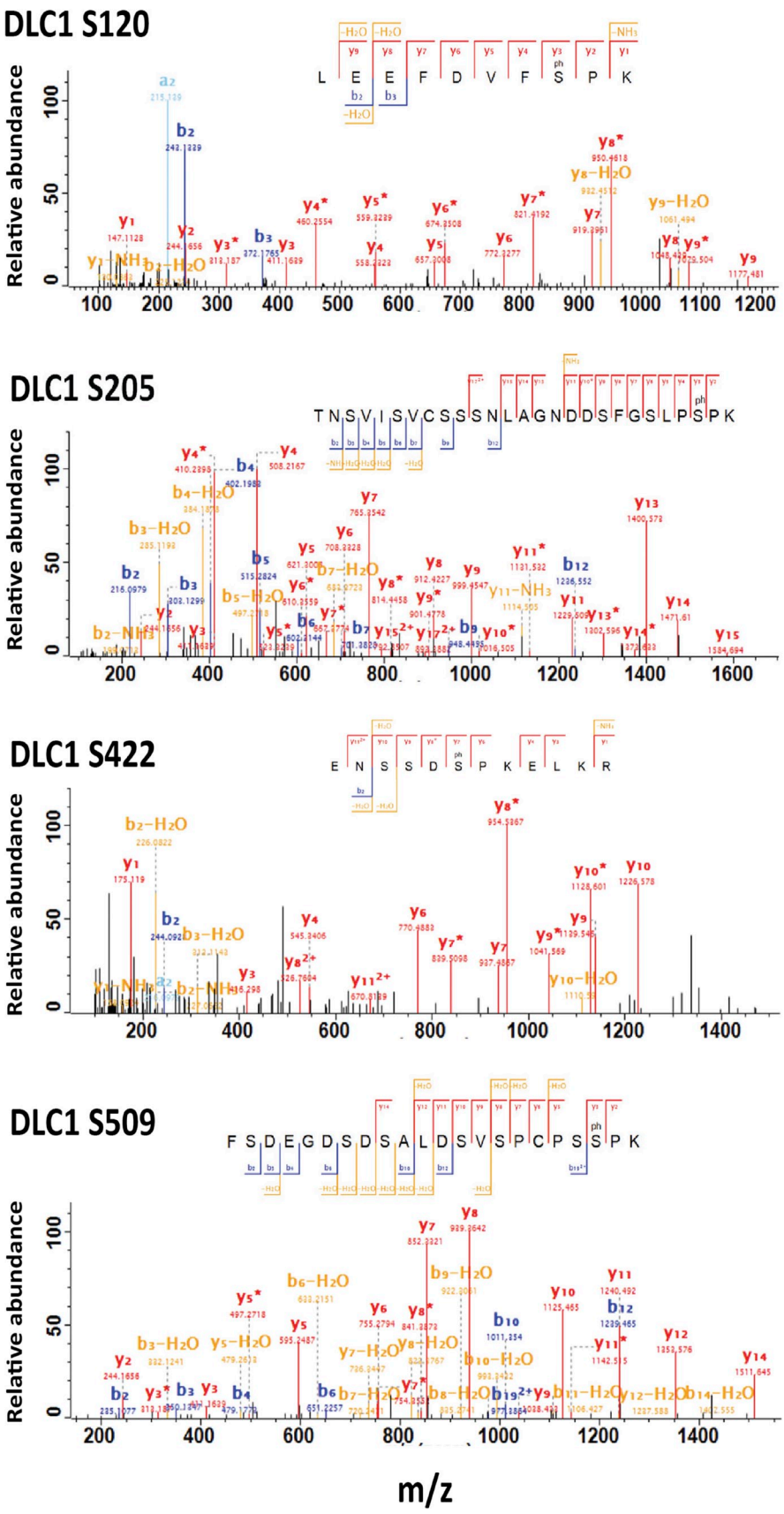

Figure S3. **DLC1 phosphopeptides identified by mass spectrometry.** Annotated MS/MS spectra are shown for the four phosphopeptides containing phosphorylated S120, S205, S422, and S509. b-Type fragments are shown in blue and y-type fragments in red. Water- and ammonia-loss peaks are shown in yellow, and neutral phosphate losses are indicated with asterisks. The fragment ions observed allow full localization of the phosphorylation sites on the Serine residues noted in each peptide. Spectra were annotated using the Viewer software of the MaxQuant 1.3.0.5 software package.

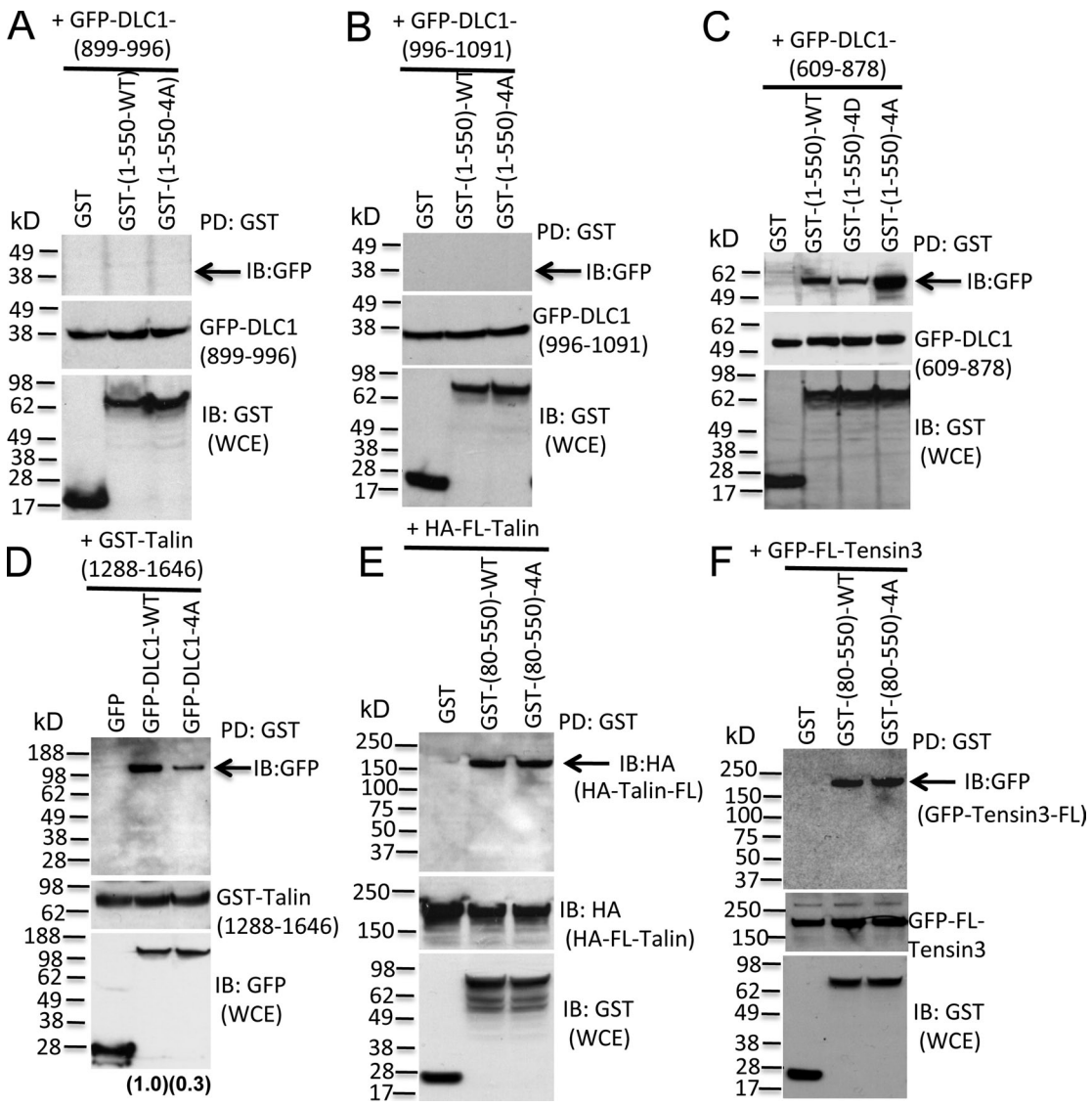

Figure S4. **Rho-GAP domain binds more strongly to DLC1(1–550)-4A mutant than to DLC1(1–550)-WT.** (A) Immunoblots from DLC1-negative A549 cells cotransfected with GFP-DLC1(899–996) and GST, GST-DLC1(1–550)-WT, or GST-DLC1(1–550)-4A constructs, pulled down by GST antibody, separated by SDS-PAGE, and immunoblotted with GFP antibody (top). WCE was immunoblotted with GFP (middle) and GST (bottom) antibodies to verify the expression of each construct. (B) Experimental conditions were similar as those in A, except the DLC1 construct differed. Immunoblots from cells cotransfected with GFP-DLC1(996–1,091) and GST, GST-DLC1(1–550)-WT or GST-DLC1(1–550)-4A constructs. (C) Immunoblots from cells cotransfected with Rho-GAP domain of DLC1 (GFP-DLC1(609–878)) and GST, GST-DLC1(1–550)-WT, GST-DLC1(1–550)-4D, or GST-DLC1(1–550)-4A constructs, pulled down, and immunoblotted with GFP antibody (top). WCE was immunoblotted with GFP (middle) and GST (bottom) antibodies to check the expression of each construct. The GST-DLC1(1–550)-4A mutant binds more efficiently to the Rho-GAP domain than do the GST-DLC1(1–550)-WT or GST-DLC1(1–550)-4D mutant. (D) Immunoblots from cells cotransfected with GST-tagged Talin(1,288–1,646) and GFP, GFP-DLC1-WT, or GFP-DLC1-4A mutant, pulled down, and detected with GFP antibody (top). WCE was immunoblotted with GST (middle) and GFP antibodies (bottom) to check the expression of each construct. GST-Talin(1,288–1,646) binds more strongly to GFP-DLC1-WT compared to GFP-DLC1-4A mutant. (E) Immunoblots from cells cotransfected with HA-tagged full-length Talin and GST, GST-DLC1(80–550)-WT, or GST-DLC1(80–550)-4A, pulled down, and immunoblotted with HA antibody (top). WCE was immunoblotted with HA (middle) and GST antibodies (bottom) to check the expression of each construct. (F) Immunoblots from cells cotransfected with GFP-tagged full-length Tensin3 and GST, GST-DLC1(80–550)-WT, or GST-DLC1(80–550)-4A, pulled down, and detected with GFP antibody (top). WCE was immunoblotted with GFP (middle) and GST antibodies (bottom) to check the expression of each construct. The immunoblots are representative of three independent experiments.

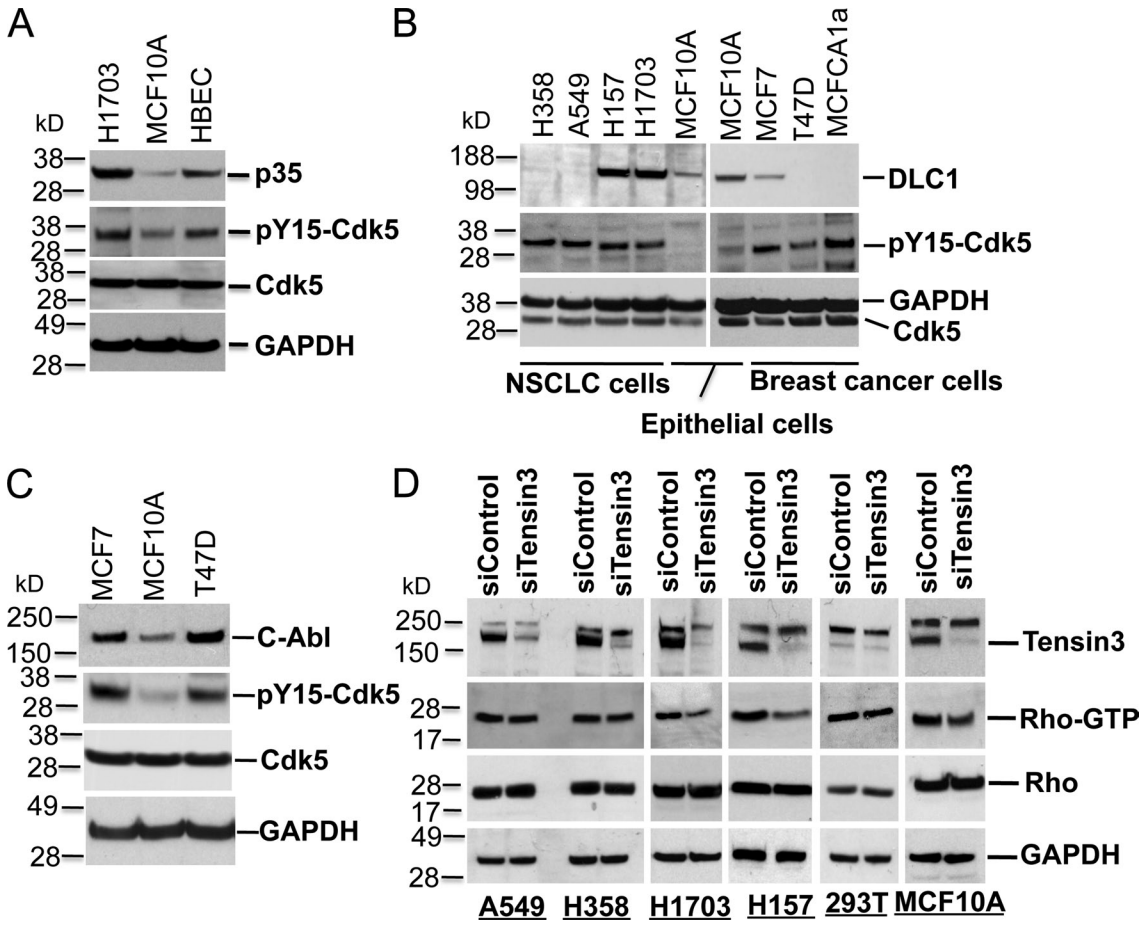

Figure S5. **Basal CDK5 kinase activity is low in the MCF10A cell line, and depletion of tensin-3 did not produce a substantial change in RhoGTP.** (A) Immunoblots for p35 (top), CDK5-pY15 (second from the top), and total CDK5 (second from the bottom), and GAPDH (bottom) in the indicated cell lines. (B) CDK5 kinase activity (as depicted by phosphorylation of Tyrosine-15 in CDK5) in the indicated cell lines. Immunoblots for DLC1 (top), CDK5-pY15 (middle), CDK5, and GAPDH (bottom) in various indicated cell lines. (C) Immunoblots for c-Abl (top), CDK5-pY15 (second from the top), CDK5 (second from the bottom), and GAPDH (bottom) in the indicated cell lines. (D) Influence of tensin-3 reduction on RhoGTP. Knockdown of Tensin-3 expression by siRNAs (top) in the indicated cell lines. RhoGTP (second from the top) and the total Rho (second from the bottom) in control siRNAs or Tensin-3 siRNA–transfected cells. GAPDH was used as a loading control (bottom). The immunoblots are representative of three independent experiments.